Engraftment of human iPS cells and allogeneic porcine cells into pigs with inactivated *RAG2* and accompanying severe combined immunodeficiency

Kiho Lee[a,1,2], Deug-Nam Kwon[b,1], Toshihiko Ezashi[a,c,1], Yun-Jung Choi[b], Chankyu Park[b], Aaron C. Ericsson[d], Alana N. Brown[a], Melissa S. Samuel[a,e], Kwang-Wook Park[a,f], Eric M. Walters[a,e], Dae Young Kim[d], Jae-Hwan Kim[g], Craig L. Franklin[d], Clifton N. Murphy[a], R. Michael Roberts[a,c,d,h,3], Randall S. Prather[a,e,3], and Jin-Hoi Kim[b,3]

[a]Division of Animal Science, [c]Bond Life Sciences Center, Departments of [d]Veterinary Pathobiology and [h]Biochemistry, and [e]National Swine Resource and Research Center, University of Missouri, Columbia, MO 65211; [b]Department of Animal Biotechnology, Konkuk University, Seoul 143-701, Korea; [g]Department of Biomedical Science, College of Life Science, CHA University, Seongnam-si, Gyeonggi-Do 463-836, Korea; and [f]Department of Animal Science and Technology, Sunchon National University, Suncheon, Jeonnam 540-742, Korea

Contributed by R. Michael Roberts, April 9, 2014 (sent for review February 19, 2014)

Pigs with severe combined immunodeficiency (SCID) may provide useful models for regenerative medicine, xenotransplantation, and tumor development and will aid in developing therapies for human SCID patients. Using a reporter-guided transcription activator-like effector nuclease (TALEN) system, we generated targeted modifications of recombination activating gene (*RAG*) 2 in somatic cells at high efficiency, including some that affected both alleles. Somatic-cell nuclear transfer performed with the mutated cells produced pigs with *RAG2* mutations without integrated exogenous DNA. Biallelically modified pigs either lacked a thymus or had one that was underdeveloped. Their splenic white pulp lacked B and T cells. Under a conventional housing environment, the biallelic *RAG2* mutants manifested a "failure to thrive" phenotype, with signs of inflammation and apoptosis in the spleen compared with age-matched wild-type animals by the time they were 4 wk of age. Pigs raised in a clean environment were healthier and, following injection of human induced pluripotent stem cells (iPSCs), quickly developed mature teratomas representing all three germ layers. The pigs also tolerated grafts of allogeneic porcine trophoblast stem cells. These SCID pigs should have a variety of uses in transplantation biology.

Stem cells show great promise for regenerative medicine. Creation of human induced pluripotent stem cells (hiPSCs), in particular, may afford sources of tissue for individualized transplantation therapy, provided that effective delivery systems and differentiation protocols can be developed. However, concerns exist about whether iPSCs, in particular, have full pluripotent potential and whether they are safe to be applied to transplantation therapy. Moreover, there is growing recognition that animal models other than rodents are needed for many biomedical applications (1, 2), including the development of procedures for establishing xenografts from whole organs and transplanted cells. Moreover, rodents are not always appropriate for mimicking some human genetic and infectious disease states, and, for some surgical and clinical monitoring purposes, rodents are simply too small to be practical (3, 4).

Rodents with severely compromised immune systems, including ones with either a mutated recombination activating gene (*RAG*) 1 (5) or *RAG2* (6) gene, have become valuable for a variety of purposes in addition to studying the development of the immune system. For example, after further genetic modifications, they can be used for the production of "humanized" rodents carrying human cell lineages (7, 8). They have proved especially useful in stem-cell biology for studies on tissue regeneration and for examining whether or not stem cells form teratomas and exhibit full pluripotency (9). Mice, however, not only have limitations in terms of size, longevity, and organ physiology but have diverged extensively from humans in various aspects of both their adaptive and innate immune systems, such that mutations in particular genes do not necessarily affect both species similarly (10). By contrast, the immune cell populations of pigs and humans are quite similar and differ in numerous respects from those of the mouse (4). Moreover, rodents show very different patterns of gene expression after inflammation compared with humans (11).

Pigs are an excellent animal model to represent some human diseases, as the two species share similar physiologies, and pigs can replicate some human diseases with higher fidelity than rodent models (3, 12). This response to immune challenge may be particularly true for diseases associated with the immune system. For example, there are two brief descriptions of a group of SCID-like pigs that arose spontaneously in a standard breeding program (13, 14). These animals were unable to produce antibodies, had atrophied lymph nodes, and lacked a thymus and B and T cells, and were also able to accept s.c. grafts of human melanoma and pancreatic carcinoma cells. However, the genetic basis of this SCID-like phenotype remains unclear. Two other groups have disrupted the X-linked porcine gene encoding *IL2RG* (interleukin 2 receptor gamma) and obtained a SCID phenotype. Suzuki et al. (15) targeted *IL2RG* in somatic cells by homologous

Significance

Pigs have many features that make them attractive as biomedical models, especially in regenerative medicine. Here, we have introduced inactivating mutations simultaneously into both alleles of the recombination activating gene (*RAG*) 2 gene in fibroblasts derived from minipigs and then used somatic-cell nuclear transfer to produce *RAG2*$^{-/-}$ cloned animals with a severe immune deficiency (SCID) phenotype and lacking T and B cells. When human induced pluripotent (iPS) cells were injected into these SCID pigs, the animals readily form teratomas representing a wide range of human tissues. Provided they can be protected from pathogens, these genetically engineered pigs could be a valuable resource as models for human patients with analogous immunodeficiencies and for testing the safety and regenerative capacity of grafts derived from iPS cells.

Author contributions: K.L., D.-N.K., and T.E. designed research; K.L., D.-N.K., T.E., A.N.B., M.S.S., K.-W.P., E.M.W., and C.N.M. performed research; K.L., D.-N.K., T.E., Y.-J.C., C.P., A.C.E., A.N.B., E.M.W., D.Y.K., Jae-Hwan Kim, and C.L.F. analyzed data; K.L., D.-N.K., T.E., R.M.R., R.S.P., and Jin-Hoi Kim wrote the paper; and R.M.R., R.S.P., and Jin-Hoi Kim supervised the project.

The authors declare no conflict of interest.

Freely available online through the PNAS open access option.

[1]K.L., D.-N.K., and T.E. contributed equally to this work.

[2]Present address: Department of Animal and Poultry Sciences, Virginia Polytechnic Institute and State University, Blacksburg, VA 24061.

[3]To whom correspondence may be addressed. E-mail: robertsrm@missouri.edu, PratherR@Missouri.edu, or jhkim541@konkuk.ac.kr.

This article contains supporting information online at www.pnas.org/lookup/suppl/doi:10.1073/pnas.1406376111/-/DCSupplemental.

recombination and used serial nuclear transfer and further breeding to generate heterozygous *IL2RG*$^{+/-}$ females and *IL2RG*$^{-/Y}$ males that were athymic and had impaired production of immune cells. The aberrant phenotype of the males could be corrected by allogeneic bone marrow transplantation. Watanabe et al. (16) used the more efficient zinc finger nuclease (ZFN) technology to knock out the same gene in fibroblasts, performed nuclear transfer, and observed an essentially identical phenotype as Suzuki et al. (15). However, they did not perform grafts on the animals.

The use of meganucleases, such as ZFNs, and transcription activator-like effector nucleases (TALENs) has permitted a highly efficient and precise means for gene targeting by introducing double-strand breaks (DSB) at preselected sites, which results in random mutations through nonhomologous end joining (NHEJ) (17, 18). ZFNs and TALENs are showing great promise for creating genetically engineered pigs (16, 19–21) although, in many cases, additional cloning or breeding steps are required to produce biallelic mutant animals without any integration of exogenous DNA because a selectable marker or transposon element is often used in association with the vector. Because pigs have a gestation length of almost 4 mo and do not reach sexual maturity until about 6 mo of age, it would be advantageous to produce biallelic mutants in the founding generation. A major goal of the present project was to target simultaneously both alleles of the autosomal *RAG2* gene. Such mutations could have value as models for several SCID-related diseases in humans, including Omenn syndrome (22, 23). RAG2 and RAG1 orchestrate the generation of antigen receptor diversity by properly regulating V(D)J rearrangements (24). In mice, inactivating mutations in *RAG2* results in impaired development of B and T cells, thus disrupting the adaptive immune system (6). *RAG2* null mice, because they are immunodeficient, are valuable for a range of purposes in transplant studies and are especially useful for generating teratomas for pluripotency assessment tests (25). Here, we report an efficient method for generating *RAG2* mutant pigs with a T-B-NK^{+} SCID phenotype: i.e., the animals lack T and B cells but possess NK cells, which supports proliferation and differentiation of hiPSC and allogeneic porcine trophoblast stem cells. In addition to being models for SCID-related diseases in humans, these pigs may be a useful translational animal model to evaluate the efficacy and safety of stem-cell engraftment, to develop surgical procedures for placement of grafts before clinical trials in humans, and to produce partially humanized swine.

Results

Targeted Mutation of RAG2 Using TALENs. Specific TALENs were designed and synthesized by Toolgen to mutate exon 2 of *RAG2* (Fig. 1*A*). The constructs coding for TALENs and a reporter were introduced into pig fibroblast cells by electroporation. This procedure provides transient expression from the vector without leading to integration of vector DNA into the host-cell genome. A reporter containing TALEN recognition sites allowed individual cells to be screened for proper expression of functional TALEN sets (26) (*SI Appendix*, Figs. S1 and S2). The efficiency of gene targeting was 42.1% (24/57), with 14% (8/57) biallelic modifications. Some of the mutations were associated with large-sized inserts/deletions (indels) that could be detected on a gel (Fig. 1*B*). The TALEN sets were specific to the targeted regions, and there was no evidence for any off-target cutting at closely matching sequences (*SI Appendix*, Fig. S3).

Interestingly, we found two different *RAG2* mutations from targeted colony no. 14, which originated from a single cell. One allelic modification was consistent throughout the cell population whereas the second (see Fig. 1) presumably occurred after the founder cell had divided. Three *RAG2* targeted colonies (no. 12, male cells with monoallelic mutation; no. 14, male cells, consisting of a mixed population of monoallelic and biallelic mutant cells; no. 32, female cells with a monoallelic mutation) were used for somatic cell nuclear transfer (SCNT) (*SI Appendix*, Fig. S4).

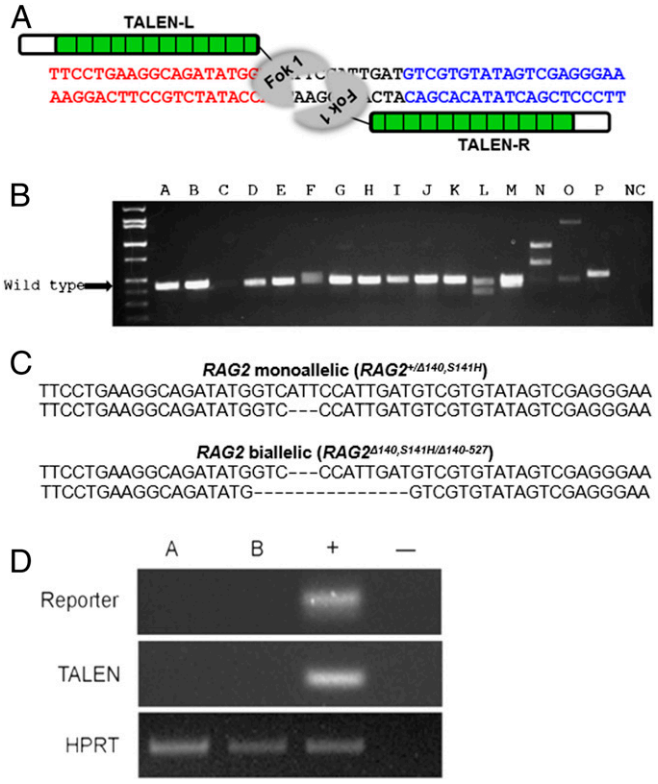

Fig. 1. Production of *RAG2* mutant pigs through use of TALENs. (*A*) TALENs designed to cause mutations in exon 2 of *RAG2*. The target site encodes a beta propeller region of the mature protein, an essential domain for functional *RAG2*. (*B*) Mono- and biallelic modification of *RAG2*. PCR products flanking TALEN binding site are shown. The absence of a PCR band of the anticipated wild-type size indicates a biallelic modification (lane N). The PCR products had been loaded on a 2.0% agarose gel. (*C*) Genotypes of the genetically engineered pigs. Pigs with both mono- and biallelic modification of *RAG2* were observed. They shared a common modification on one allele, but a significant proportion possessed a mutated second allele. (*D*) Absence of exogenous DNA in *RAG2* mutants. Exogenous DNA could not be amplified after TALEN-mediated targeting (A, monoallelic; B, biallelic). The PCR products had been loaded on 2.0% agarose gel.

Production of RAG2 Mutant Minnesota Minipigs. *RAG2* mutant pigs were produced by SCNT from the targeted fibroblast cells. In all, nine embryo transfers were performed. All of the surrogates had a full-term pregnancy (*SI Appendix*, Table 1). The first group of piglets (1–3), derived from the male cell lines no. 12 and no. 14, were maintained under standard housing conditions and examined for SCID phenotype. The second group (4–6), all from no. 14, were kept as free as possible from potential pathogens and used to support growth of teratomas whereas those piglets from litters 7–9 (from female line no. 32), also kept under clean conditions, were set aside for future breeding. As, anticipated, genotyping of piglets from targeted colony no. 14 revealed that some piglets had monoallelic and others biallelic modifications of *RAG2* (Fig. 1*C*). The monoallelic mutants (*RAG2*$^{+/\Delta 140,\ S141H}$) had a deletion of 3 bases in adjacent codons, resulting in a single amino acid deletion and one amino acid replacement (S→H) in one allele. The biallelic mutants (*RAG2*$^{\Delta 140,S141H/\Delta 140–527}$) had the same modification on one allele plus a premature stop codon on the second allele due to the deletion of 14 nucleotides.

The first three litters provided 16 piglets. Three were stillborn (two monoallelic and one biallelic), and six (four monoallelic and two biallelic) died during the first week after birth, presumably resulting from SCNT-induced abnormalities rather than immune deficiency. The surviving eight pigs (four monoallelic and four

biallelic) were compared with two wild-type control pigs, which were euthanized when they were 17 and 29 d of age. Integration of exogenous DNA was not detected in any of the genetically modified animals. Specifically, TALENs and the reporter constructs were absent as indicated by PCR (Fig. 1*D*). The lack of integration was anticipated, as the constructs coding for the TALENs and reporter were designed to be transiently introduced into the cells and eventually lost. Additionally there was no sign of red fluorescence, which would have indicated persistence of the vector in the pigs or fibroblast cells derived from the animals.

SCID-Like Phenotype in Biallelic RAG2 Mutants. The genotype of the *RAG2* biallelic mutants ($RAG2^{\Delta 140,S141H/\Delta 140-527}$) suggested that the piglets would have a nonfunctional *RAG2*, as a stop codon had been introduced into one allele whereas both the deleted and replaced amino acids on the other allele are highly conserved and presumed essential across various species (*SI Appendix*, Fig. S5). A SCID-like phenotype was therefore anticipated in these pigs but not in the $RAG2^{+/\Delta 140,\ S141H}$ heterozygotes.

Birth weights of the *RAG2* mono- and biallelic pigs were similar to those of wild-type control animals. However, 2 wk after birth, the wild-type and $RAG2^{+/\Delta 140,\ S141H}$ pigs in the standard housing environment began to gain weight faster than the $RAG2^{\Delta 140,S141H/\Delta 140-527}$ mutants, whose growth had begun to slow appreciably (Fig. 2 *A* and *B*). Such a neonatal failure to gain weight is commonly observed in human SCID infants (27, 28). Skin-derived fibroblast cells from the $RAG2^{\Delta 140,S141H/\Delta 140-527}$ pigs proliferated at a rate comparable with those from the two groups of pigs, indicating that cellular proliferation was probably not the cause of the failure to gain weight (Fig. 2*C*). The $RAG2^{\Delta 140,S141H/\Delta 140-527}$ pigs had appeared to eat normally, and, at necropsy, their stomachs contained feed. On the other hand, they began to show an elevated body temperature and shivering, by the time they were 2 wk old, and all either died or were euthanized before they had reached 29 d.

Postmortem analysis showed that the $RAG2^{\Delta 140,S141H/\Delta 140-527}$ animals displayed mild infiltration of lymphoid cells in kidney, liver, and lung (Fig. 2*D*) and an increased abundance of mRNA for genes indicative of inflammation and apoptosis in the spleen compared with age-matched wild-type animals (*SI Appendix*, Figs. S6 and S8). Signs of apoptosis were further confirmed by TUNEL staining (Fig. 2*E* and *SI Appendix*, Fig. S7).

All four $RAG2^{+/\Delta 140,\ S141H}$ pigs examined had thymus glands comparable in size with those recovered from the two wild-type control pigs (Fig. 3*A*). By contrast, three of four $RAG2^{\Delta 140,S141H/\Delta 140-527}$ pigs lacked a thymus whereas that of the fourth was very small compared with that of an age-matched (day 29) control pig (Fig. 3*A* and *SI Appendix*, Fig. 9). In addition, the spleens of the biallelic mutants were smaller than those of the control pigs (Fig. 3*B*) (weights 8.32 g, 6.49 g, and 1.88 g in wild-type, monoallelic, and biallelic mutants, respectively). The white pulp of spleens from $RAG2^{\Delta 140,S141H/\Delta 140-527}$ mutants was markedly hypoplastic and lacked germinal centers and periarteriolar lymphoid sheaths (*SI Appendix*, Fig. S10). Only a few cells carrying markers for B cells ($CD79A^+$) and T cells ($CD3^+$) were present, and these cells were scattered throughout the sections (Fig. 3*C*). In contrast, B- and T-cell numbers from the $RAG2^{+/\Delta 140,S141H}$ pigs appeared to be normal. Although NK cells were present in all animals, their numbers in the $RAG2^{\Delta 140,S141H/\Delta 140-527}$ pig spleen appeared lower than in the other two groups (Fig. 3*C*). Macrophages were detected in all animals (*SI Appendix*, Fig. S11), but flow cytometry confirmed that $RAG2^{\Delta 140,S141H/\Delta 140-527}$ pigs lacked mature $CD21^+$ B and $CD3^+$ T cells (Fig. 3*D*). Together, these results confirmed a consistent T-B-NK^+ immunodeficient phenotype in the $RAG2^{\Delta 140,S141H/\Delta 140-527}$ pigs.

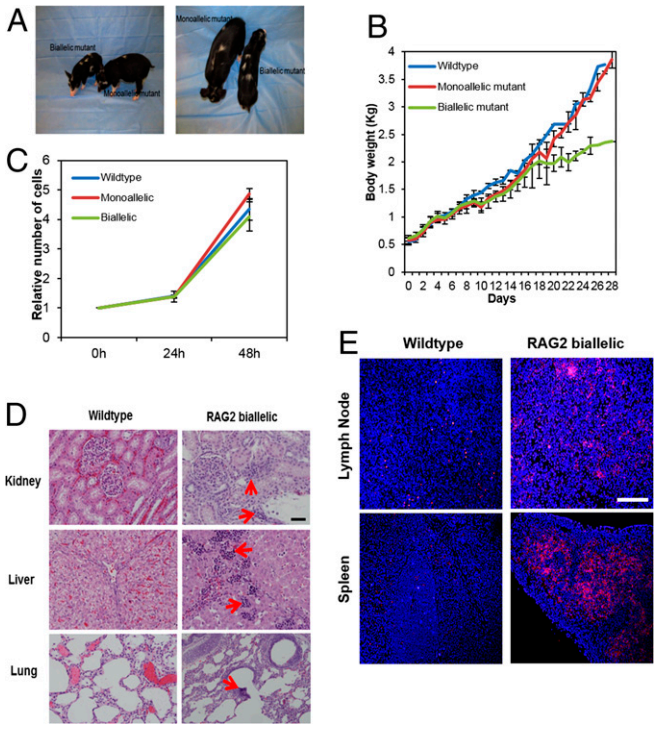

Fig. 2. Failure to thrive phenotype in $RAG2^{\Delta 140,S141H/\Delta 140-527}$ pigs. (*A*) *RAG2* bi- and monoallelic mutants at 4 wk of age. (*B*) Body weight gain of control, monoallelic, and biallelic mutant pigs over time after birth when they were maintained under standard housing conditions. Error bars indicate SD. Statistical treatment of the data was not possible because, at d 28, only one pig from the biallelic group remained alive. (*C*) Proliferation of fibroblast cells derived from wild-type and mono- and biallelic *RAG2* $RAG2^{\Delta 140,S141H/\Delta 140-527}$ pigs. Cell numbers were measured at 24 h and 48 h. No differences were noted in the growth rates of the cells from the three sources ($P > 0.05$). (*D*) Abnormal lymphocyte infiltration into kidney, liver, and lung (arrowed) of $RAG2^{\Delta 140,S141H/\Delta 140-527}$ pigs. (Scale bar: 100 μm.) (*E*) Apoptosis in spleen and lymph node of $RAG2^{\Delta 140,S141H/\Delta 140-527}$ pigs shown by TUNEL staining (pink). (Scale bar: 500 μm.)

Successful and Efficient Teratoma Formation from Human iPSCs. To test whether the $RAG2^{\Delta 140,S141H/\Delta 140-527}$ pigs would support proliferation and differentiation of human iPSCs, we injected pigs s.c. with cells from a potentially pluripotent cell line that had been generated from human umbilical cord fibroblasts by reprogramming with nonintegrating plasmid vectors to determine whether the cells would give rise to teratomas. Before injection, the cells had been alkaline phosphatase-positive and expressed the pluripotent markers [POU class 5 homeobox 1 (POU5F1), Nanog homeobox (NANOG), stage specific embryonic antigen 3 (SSEA-3)] (*SI Appendix*, Fig. S12 *C–E*). Because the $RAG2^{\Delta 140,S141H/\Delta 140-527}$ pigs were immunocompromised, the second group of newly born piglets used for this experiment were housed independently, and all personnel contacting the animals wore protective personal equipment (PPE) in an attempt to minimize pathogen exposure. On day 1 of the experiment, either 5 or 10 million cells were injected s.c. close to the base of the right ear and on the animal's left flank (biallelic pigs, $n = 3$; monoallelic pigs, $n = 2$). One biallelic mutant pig died of unknown cause on day 7 without showing any sign of tumor formation, but the other two developed tumors at each of the two injection sites. Tumor formation occurred rapidly compared with the usual time span of many weeks in SCID mice. A palpable tumor was observed by day 12 below the ear site of one biallelic mutant pig that had received an injection of 10 million cells (Fig. 4*A* and *SI Appendix*, Fig. S13). By day 28, this tumor

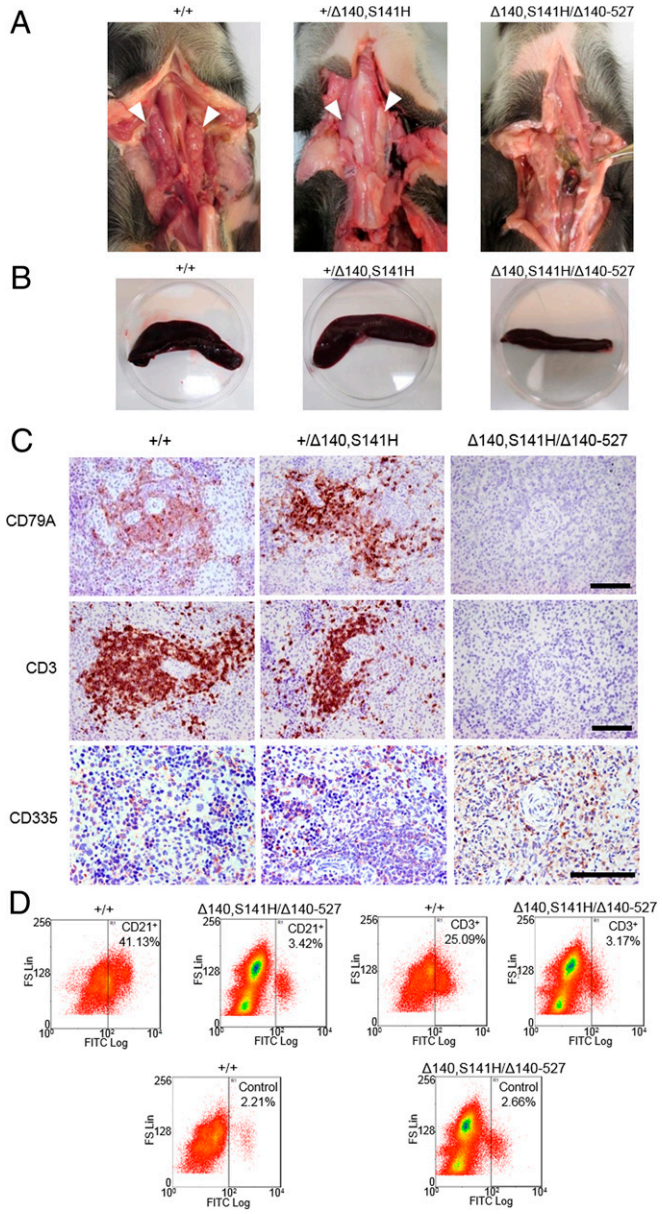

Fig. 3. SCID-like phenotype in *RAG2* biallelic $RAG2^{\Delta 140,S141H/\Delta 140-527}$ pigs. (*A*) Absence of thymus in the biallelic animals. The thymuses of monoallelic mutants were similar in size to those of the wild type. (*B*) Comparison of spleens from wild-type and mono- and biallelic mutant pigs. (*C*) SCID phenotype in the biallelic mutant pigs as revealed by comparison of the distribution (red/brown staining by specific antibodies) of CD79A (B cells), CD3 (T cells), and NK cells (CD335) in the spleen compared with monoallelic and wild-type pigs of the same age. (Scale bar: 100 μm.) (*D*) Flow cytometry of spleen cells showing a significant reduction in B ($CD21^+$) and T ($CD3^+$) cells in the spleen of *RAG2* biallelic mutant compared with wild-type pigs. Only 2–3% of splenocytes from biallelic mutants were positive for B-cell or T-cell markers, roughly equivalent to the fluorescence observed with an isotype control antibody.

was capsulated, solid, and partly cystic (size, 3.4 × 2.5 cm; weight, 3.6 g) (Fig. 4 *A* and *B*), and appeared to have caused no ill effects to the host. At necropsy, it was dissected into five pieces, and sections of tissues were examined by H&E staining. Each tumor section contained a disorganized mixture of tissues (Fig. 4*C*). Striated muscle (mesoderm) (Fig. 4 *C* and *E*) was particularly evident and formed randomly distributed islands of tissue throughout the tumor. Various other areas comprised epithelium-like cells organized into glandular-like structures. They included secretory epithelia: i.e., epithelium with goblet cells (endoderm) (Fig. 4*D*) and neural epithelium (ectoderm) (Fig. 4*F*). General histological assessments were confirmed by immunohistochemical analysis with antibodies against CTNNB1 and VWF [β-catenin and von Willebrand factor (VWF): endoderm] (Fig. 4 *G* and *J*), DES and ACTG2 (desmin and smooth muscle actin: mesoderm) (Fig. 4 *H* and *K*), and GFAP and ENO2 (glial fibrillary acidic protein and neuron-specific enolase: ectoderm) (Fig. 4 *I* and *L*). Cells positive for the markers of hematopoietic lineage and potentially pluripotent cells were also noted (Fig. 4 *M*–*O*). The second biallelic mutant pig formed slower-growing, smaller tumors (0.75 g and 0.35 g) at the ear site (where 5 million cells were injected) and flank (10 million cells injected) by 7.5 wk. An additional tumor was found in the peritoneal cavity of the second pig near the injection site on the left flank. Proportionately less muscle tissue and more cystic structures (*SI Appendix*, Fig. S14*A*) were observed in tumors from the second pig, but derivatives of all three germ layers were still present (*SI Appendix*, Fig. S14 *B*–*D*). These differences in teratoma characteristics cannot be attributed to the iPSC source because the same cells were used for each pig. The tumors were also clearly of human and not porcine origin, as amplicons from human-specific *MFN1* (mitochondrial mitofusin-1) were successfully amplified from the DNA of the human iPSC line and its derived teratoma but not from DNA of the mutant pig (*SI Appendix*, Fig. S15).

To explore whether $RAG2^{\Delta 140,S141H/\Delta 140-527}$ pigs could accept allogeneic pig cells, we injected what we have inferred previously to be porcine trophoblast stem cells, which, in nude mice, had given rise to solid tumors comprised largely of packed epithelial layers, with islands of striated muscle tissue near the periphery (29). These same cells provided a somewhat similar, encapsulated tumor in pigs by day 17. This tumor, like the ones from mouse, was comprised predominantly of layers of epithelial tissue. Eosinophilic material was often present between the cell layers (*SI Appendix*, Fig. S16), and regions of striated muscles were detectable near the margins of the tumor (*SI Appendix*, Fig. S16 *A* and *B*). No tumors developed in the monoallelic mutant pigs.

Discussion

Pigs, due to their similarities to humans, have great advantages over rodents as a translational model in advancing stem-cell therapies. They are likely to provide improved means for development of cell delivery and surgical protocols, for gauging the likely success of grafts, and for judging whether procedures are likely to be safe. However, medical applications of genetically engineered large animals have generally been limited because it has been difficult and expensive to provide the requisite numbers. One important aspect of the present study is that it demonstrates the feasibility of producing genetically engineered pigs, free of exogenous DNA and with both alleles mutated, relatively quickly and at minimum cost. The $RAG2^{\Delta 140,S141H/\Delta 140-527}$ pigs described may not only be valuable for experiments in regenerative medicine but may also represent a step forward in developing swine as model for severe immunodeficiency diseases in humans.

There were clearly differences in phenotype between $RAG2^{\Delta 140,S141H/\Delta 140-527}$ pigs and *RAG2* mutant mice. The latter have a small, but nevertheless detectable, thymus (6) whereas three of the four mutant pigs lacked a thymus completely and the fourth had one that was extremely underdeveloped, as was also observed in pigs lacking an intact *IL2RG* gene (15, 16). The lack of B and T cells is analogous to mouse, rat, and rare human *RAG* mutants (6, 30, 31), but, as with the porcine *IL2RG* knock-outs and human patients, $RAG2^{\Delta 140,S141H/\Delta 140-527}$ pigs failed to thrive when kept under standard housing conditions. Fibroblasts from the pigs proliferated normally, suggesting that there was not an intrinsic growth defect in the animals. Infiltration of innate lymphoid cells was detected in a number of tissues of the $RAG2^{\Delta 140,S141H/\Delta 140-527}$ pigs although the specific type of

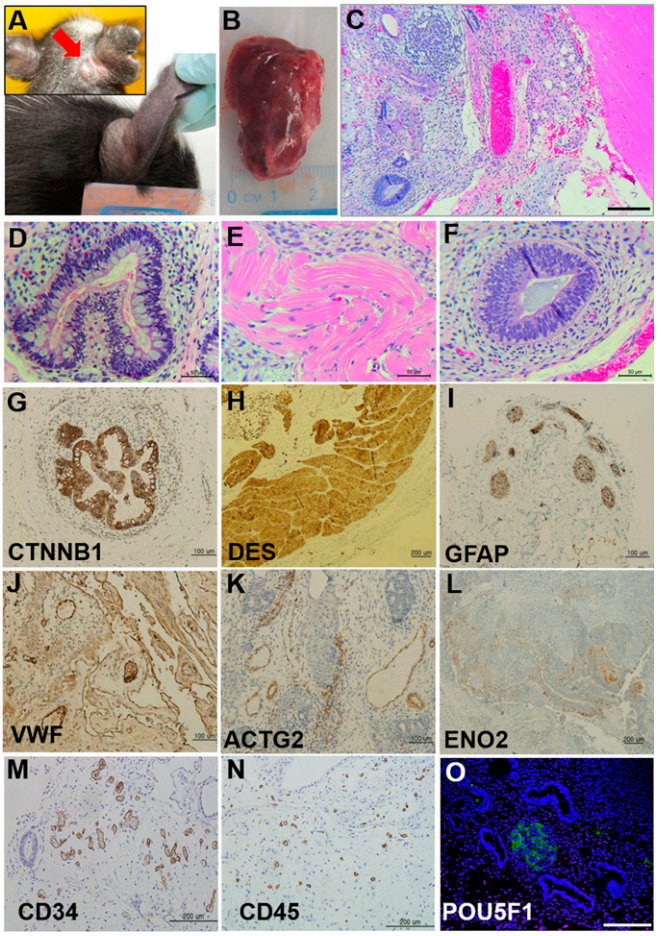

Fig. 4. Teratoma formation in $RAG2^{\Delta 140,S141H/\Delta 140-527}$ pigs. (*A*) External view of a tumor at day 16 (*Upper Inset*, red arrow) and 4 wk (*Lower*) after injection of 10 million cells below the ear. (*B*) Gross morphology of the capsulated tumor collected from the injection site. (*C*–*O*) Histological examination of the tumors. Sections were stained by H&E (*C*–*F* collected from the tumor at the ear site) and for a range of diagnostic antigen immunohistochemistry (*G*–*O*). *C* is viewed at a lower magnification of the tissues. (Scale bar: 200 μm.) (*M* and *N*) Cells positive for hematopoietic markers were present within the teratoma. (*O*) Presence of undifferentiated $POU5F1^{+}$ cells in the teratoma (green fluorescence, POU5F1; blue, DAPI stain for DNA). (Scale bar: 200 μm.)

lymphoid cells was not analyzed in this study. These findings suggest that the biallelic $RAG2^{\Delta 140,S141H/\Delta 140-527}$ pigs were more susceptible to inflammatory disease, most likely caused by pathogens, than controls and monoalleic animals, as was expected from their SCID genotype. After observing these pathological symptoms, $RAG2^{\Delta 140,S141H/\Delta 140-527}$ animals were subsequently housed individually, and all caretaker staff wore full PPE to minimize contact with human pathogens. Although this environment did not constitute a pathogen-free environment, it did allow $RAG2^{\Delta 140,S141H/\Delta 140-527}$ pigs to be maintained in what appeared to be a healthy condition for up to 8 wk, a time sufficiently long to complete the transplant experiments. The $RAG2^{\Delta 140,S141H/\Delta 140-527}$ pigs kept under standard housing conditions, like *IL2RG* knock-out pigs, exhibited a failure to thrive (FTT) phenotype comparable with that observed in humans. $Prkdc^{-/-}$ rats with a SCID phenotype are also growth retarded (32), but, in this case, the growth retardation begins during early embryonic/fetal development and does not replicate the human FTT phenotype particularly well. It still remains unclear whether or not infections, apoptosis, or inflammation in $RAG2^{\Delta 140,S141H/\Delta 140-527}$ pigs accounts for the FTT phenotype.

Immunohistological analysis confirmed a wide range of tissue types in the teratoma derived from human iPSCs. Specifically, the tumors displayed cells positive for GFAP, indicating that the teratomas were of the so-called mature type (33). In addition, cells positive for VWF were present, suggesting the presence of hematopoietic stem cells (34). The ability of $RAG2^{\Delta 140,S141H/\Delta 140-527}$ pigs to support the rapid growth of well-developed human teratomas representing a wide range of tissue types, and to permit the growth of tumors from an allogeneic porcine trophoblast cell line, suggests that such mutant animals could have considerable value in regenerative medicine. Large animals with a SCID phenotype have arisen occasionally in breeding programs (13, 14, 35), and *IL2RG* knock-out pigs have also been genetically engineered (15, 16). At least some of these animals appear to permit limited engraftment of both porcine and human cells. What our studies demonstrate is the capacity of undifferentiated human stem cells to differentiate rapidly into a wide range of cell types representative of the three germ layers in a porcine host, which further emphasizes the potential value of the *RAG2* knockout model as an alternative to immunodeficient rodents in regenerative medicine. On the other hand, the technical challenge of maintaining these animals free of pathogens for extended periods of time is likely to become an important issue. Although the teratoma experiments were completed in a few weeks, much longer periods will probably be required for full maturation and functional integration of grafts into whole organs. Also, most human patients requiring grafts are likely to be adults so that fully mature animals would be required to mimic the clinical scenario. These considerations may place limitations on the value of this pig model.

In summary, we have generated SCID pigs by a relatively efficient process and demonstrated that the animals could support the growth of mature teratomas from human pluripotent stem cells. Provided that such pigs can be maintained in an environment where exposure to pathogens is minimized and that the animals do not die prematurely of SCID-related complications, they are ideal candidates for testing stem-cell therapies, whole-organ transplants, and other procedures where immune tolerance in a large animal is desirable. Such genetically engineered pigs may be a valuable resource for the biomedical community and are available via the National Swine Resource and Research Center (http://nsrrc.missouri.edu/).

Materials and Methods

A more complete description of procedures used in the study is provided in *SI Appendix, SI Materials and Methods*.

Production of Pigs Carrying Targeted Mutation of RAG2. Mutated pigs were produce by targeted modification of *RAG2* in fetal fibroblast cells followed by SCNT and embryo transfer. Constructs coding for TALENs and a reporter were electroporated into fetal-derived fibroblast cells. After 48 h, transfected cells expressing the green fluorescent protein were sorted into individual wells of a 96-well plate at an estimated dilution of a single cell per well. Targeted modification of *RAG2* was screened by amplifying a genomic DNA fragment flanking the TALEN cutting sites followed by sequencing the PCR products. After screening and ensuring lack of off-site mutations, cells carrying targeted modification of *RAG2* were used for SCNT. The polar body, along with a portion of the adjacent cytoplasm of oocyte, presumably containing the metaphase II plate, was removed, and a donor cell was placed in the perivitelline space as described previously (36). The reconstructed embryos were then electrically porated to fuse the donor cell with the oocyte and then chemically activated (37). The activated embryos were incubated in Porcine Zygote Medium 3 (PZM3) (38) with 0.5 μM Scriptaid (S7817; Sigma-Aldrich) for 14–16 h. Embryos were then washed to remove the Scriptaid and cultured in PZM3 until they were transferred into the oviducts of surrogate pigs. A total of nine embryo transfers were performed for the study, resulting in birth of 22 live piglets (*SI Appendix*, Fig. S1). All experiments involving animals were approved by the University of Missouri Institutional Animal Care and Use Committee.

Generation of iPSCs from Human Umbilical Cord Fibroblasts with Episomal Vectors. Human umbilical cord tissues from two individuals were collected, with informed consent, in University Hospital (University of Missouri) with approval from the University of Missouri Health Sciences Institutional Review Board (no. 1201132). The fibroblast outgrowths from umbilical cords were reprogrammed with nonintegrating episomal vectors by a protocol developed by Okita et al. (39). Two iPSC lines were examined for expression of alkaline phosphatase and sets of pluripotent markers (POU5F1, NANOG, SSEA-3) (40).

Teratoma Formation and Analysis. Two human iPSC lines and porcine cells with a trophoblast phenotype (29) were injected with either 5 or 10 million cells per site. Tumors were collected following euthanasia 4–7.5 wk after cell injections and portions fixed in 4% (wt/vol) formaldehyde and embedded in paraffin wax. Some tissue was retained for analysis of DNA and for extraction of RNA. Histochemical and immunohistochemical analyses were performed on 5-μm sections on glass slides to identify various tissue types in the tumors. The extracted genomic DNA was amplified with primers for human specific mitochondrial mitofusin 1 gene (*MFN1*) by PCR to ensure that the tumors that developed in the pigs injected with the human cells were of human origin.

ACKNOWLEDGMENTS. We thank Amanda J. Stephens, MD, and Danny J. Schust, MD, for providing the human umbilical cords that generated the iPS cells. We also acknowledge technical assistance provided by Lee Spate, Mike L. Linville, Keith Giroux, Bethany Redel, and Ben Beaton. We also thank Dr. Kevin Wells for his expert consultation. This work was supported by the Woo Jang-Choon Project (PJ007849) and Next Generation of Biogreen 21 (PJ009107) from the Rural Development Administration, Republic of Korea, and the National Institutes of Health (NIH) to the National Swine Resource and Research Center [U42OD011140 (to R.S.P.)]. Additional support was from NIH Grants R01HD067759 and R01HD069979 (to R.M.R. and T.E.) and the Food for the 21st Century Program at the University of Missouri (R.S.P. and R.M.R.).

1. Plews JR, Gu M, Longaker MT, Wu JC (2012) Large animal induced pluripotent stem cells as pre-clinical models for studying human disease. *J Cell Mol Med* 16(6): 1196–1202.
2. Harding J, Roberts RM, Mirochnitchenko O (2013) Large animal models for stem cell therapy. *Stem Cell Res Ther* 4(2):23.
3. Walters EM, Prather RS (2013) Advancing swine models for human health and diseases. *Mo Med* 110(3):212–215.
4. Meurens F, Summerfield A, Nauwynck H, Saif L, Gerdts V (2012) The pig: A model for human infectious diseases. *Trends Microbiol* 20(1):50–57.
5. Mombaerts P, et al. (1992) RAG-1-deficient mice have no mature B and T lymphocytes. *Cell* 68(5):869–877.
6. Shinkai Y, et al. (1992) RAG-2-deficient mice lack mature lymphocytes owing to inability to initiate V(D)J rearrangement. *Cell* 68(5):855–867.
7. Brehm MA, Shultz LD, Luban J, Greiner DL (2013) Overcoming current limitations in humanized mouse research. *J Infect Dis* 208(Suppl 2):S125–S130.
8. Shultz LD, Ishikawa F, Greiner DL (2007) Humanized mice in translational biomedical research. *Nat Rev Immunol* 7(2):118–130.
9. Cunningham JJ, Ulbright TM, Pera MF, Looijenga LH (2012) Lessons from human teratomas to guide development of safe stem cell therapies. *Nat Biotechnol* 30(9): 849–857.
10. Mestas J, Hughes CC (2004) Of mice and not men: Differences between mouse and human immunology. *J Immunol* 172(5):2731–2738.
11. Seok J, et al.; Inflammation and Host Response to Injury, Large Scale Collaborative Research Program (2013) Genomic responses in mouse models poorly mimic human inflammatory diseases. *Proc Natl Acad Sci USA* 110(9):3507–3512.
12. Whyte JJ, Prather RS (2011) Genetic modifications of pigs for medicine and agriculture. *Mol Reprod Dev* 78(10-11):879–891.
13. Basel MT, et al. (2012) Human xenografts are not rejected in a naturally occurring immunodeficient porcine line: A human tumor model in pigs. *Biores Open Access* 1(2): 63–68.
14. Ozuna AG, et al. (2013) Preliminary findings of a previously unrecognized porcine primary immunodeficiency disorder. *Vet Pathol* 50(1):144–146.
15. Suzuki S, et al. (2012) Il2rg gene-targeted severe combined immunodeficiency pigs. *Cell Stem Cell* 10(6):753–758.
16. Watanabe M, et al. (2013) Generation of interleukin-2 receptor gamma gene knockout pigs from somatic cells genetically modified by zinc finger nuclease-encoding mRNA. *PLoS ONE* 8(10):e76478.
17. Urnov FD, et al. (2005) Highly efficient endogenous human gene correction using designed zinc-finger nucleases. *Nature* 435(7042):646–651.
18. Miller JC, et al. (2011) A TALE nuclease architecture for efficient genome editing. *Nat Biotechnol* 29(2):143–148.
19. Hauschild J, et al. (2011) Efficient generation of a biallelic knockout in pigs using zinc-finger nucleases. *Proc Natl Acad Sci USA* 108(29):12013–12017.
20. Carlson DF, et al. (2012) Efficient TALEN-mediated gene knockout in livestock. *Proc Natl Acad Sci USA* 109(43):17382–17387.
21. Tan W, et al. (2013) Efficient nonmeiotic allele introgression in livestock using custom endonucleases. *Proc Natl Acad Sci USA* 110(41):16526–16531.
22. Villa A, Santagata S, Bozzi F, Imberti L, Notarangelo LD (1999) Omenn syndrome: A disorder of Rag1 and Rag2 genes. *J Clin Immunol* 19(2):87–97.
23. Schwarz K, et al. (1996) RAG mutations in human B cell-negative SCID. *Science* 274(5284):97–99.
24. Oettinger MA, Schatz DG, Gorka C, Baltimore D (1990) RAG-1 and RAG-2, adjacent genes that synergistically activate V(D)J recombination. *Science* 248(4962):1517–1523.
25. Carey BW, et al. (2009) Reprogramming of murine and human somatic cells using a single polycistronic vector. *Proc Natl Acad Sci USA* 106(1):157–162.
26. Kim Y, et al. (2013) A library of TAL effector nucleases spanning the human genome. *Nat Biotechnol* 31(3):251–258.
27. Hague RA, Rassam S, Morgan G, Cant AJ (1994) Early diagnosis of severe combined immunodeficiency syndrome. *Arch Dis Child* 70(4):260–263.
28. Barron MA, et al. (2011) Increased resting energy expenditure is associated with failure to thrive in infants with severe combined immunodeficiency. *J Pediatr* 159(4): 628–632, e1.
29. Ezashi T, Matsuyama H, Telugu BP, Roberts RM (2011) Generation of colonies of induced trophoblast cells during standard reprogramming of porcine fibroblasts to induced pluripotent stem cells. *Biol Reprod* 85(4):779–787.
30. Zschemisch NH, et al. (2012) Zinc-finger nuclease mediated disruption of Rag1 in the LEW/Ztm rat. *BMC Immunol* 13:60.
31. Facchetti F, Blanzuoli L, Ungari M, Alebardi O, Vermi W (1998) Lymph node pathology in primary combined immunodeficiency diseases. *Springer Semin Immunopathol* 19(4): 459–478.
32. Mashimo T, et al. (2012) Generation and characterization of severe combined immunodeficiency rats. *Cell Rep* 2(3):685–694.
33. Gu S, Wu YM, Hong L, Zhang ZD, Yin MZ (2011) Glial fibrillary acidic protein expression is an indicator of teratoma maturation in children. *World J Pediatr* 7(3): 262–265.
34. Knapp DJ, Eaves CJ (2014) Control of the hematopoietic stem cell state. *Cell Res* 24(1): 3–4.
35. Meek K, et al. (2009) SCID dogs: Similar transplant potential but distinct intra-uterine growth defects and premature replicative senescence compared with SCID mice. *J Immunol* 183(4):2529–2536.
36. Lai L, Prather RS (2003) Production of cloned pigs by using somatic cells as donors. *Cloning Stem Cells* 5(4):233–241.
37. Macháty Z, Wang WH, Day BN, Prather RS (1997) Complete activation of porcine oocytes induced by the sulfhydryl reagent, thimerosal. *Biol Reprod* 57(5):1123–1127.
38. Yoshioka K, Suzuki C, Tanaka A, Anas IM, Iwamura S (2002) Birth of piglets derived from porcine zygotes cultured in a chemically defined medium. *Biol Reprod* 66(1): 112–119.
39. Okita K, et al. (2011) A more efficient method to generate integration-free human iPS cells. *Nat Methods* 8(5):409–412.
40. Ezashi T, et al. (2009) Derivation of induced pluripotent stem cells from pig somatic cells. *Proc Natl Acad Sci USA* 106(27):10993–10998.